International Journal of Chemical, Materials and Biomolecular Sciences
ISSN: 2415-6620
Vol:12, No:1, 2018

Non-Circular Carbon Fiber Reinforced Polymers Chainring Failure Analysis

A. Elmikaty, Z. Thanawarothon, L. Mezeix

***Abstract*—**This paper presents a finite element model to simulate the teeth failure of non-circular composite chainring. Model consists of the chainring and a part of the chain. To reduce the size of the model, only the first 11 rollers are simulated. In order to validate the model, it is firstly applied to a circular aluminum chainring and evolution of the stress in the teeth is compared with the literature. Then, effect of the non-circular shape is studied through three different loading positions. Strength of non-circular composite chainring and failure scenario is investigated. Moreover, two composite lay-ups are proposed to observe the influence of the stacking. Results show that composite material can be used but the lay-up has a large influence on the strength. Finally, loading position does not have influence on the first composite failure that always occurs in the first tooth.

***Keywords*—**CFRP, composite failure, FEA, non-circular chainring.

I. Introduction

CARBON fiber reinforced polymer (CFRP) usage within aerospace, structural engineering, land transports and sport industries have increased significantly over the past 40 years. Due to their high specific strength, gain of mass is expected. Although CFRP present better mechanical properties than aluminum, they are very sensitive to impact [1]-[6] and edge damage [7]-[9]. Indeed, the CFRP strength can be considerably reduced after low velocity impact. For example, it was observed a decrease of about 25% on the ultimate tensile strength after an impact energy of 6.8 J [10]. Composites are largely used for sport equipment to increase their performance. CFRP replace wood for tennis racquets and baseball bats [11] and replace steel for golf clubs to reduce the weight and to increase the ball exit velocity [12]. Board sports as snowboarding, surfing or skateboarding take advantage of composite material to increase the bending and torsion stiffness of the board [13]. CFRP are largely used in competition cycling especially for the frame to obtain a high stiffness and strength structure at low weights [14]-[16]. Impact from stones or the chain has been experimentally measured on a mountain bike [17]. Due to the low energy of impact no structural damage had been expected. Chainring can be manufactured of either an aluminum alloy or CFRP (Fig. 1 (a)) and can be circular or not [18]. Indeed, average crank power output can be increased by using non-circular chainrings [19], [20]. Wiggins won the Tour de France in 2011 with an oval metallic rings and C. Froome with an osymetric metallic chainrings in 2013. However, non-circular carbon composite chainring is not yet used. Indeed, non-circular carbon woven/epoxy chainring with a $[45_2/0/45_2/0/45_2/0/45_2]$ lay-up for a thickness of 2 mm had shown teeth failure during professional cycling. Moreover, the teeth failure appears always at the same location (Fig. 1 (a)). Two types of failure were observed (Fig. 1 (b)); teeth breaking through its cross-section (1) and plies snatching (2).

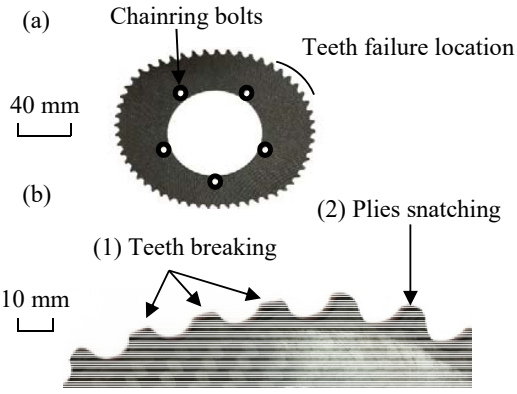

Fig. 1 Typical (a) shape and (b) teeth failure of non-circular CFRP chainring

To the best of our knowledge, failure of non-circular composite chainring has not been investigated in detail yet. Therefore in this paper, a finite element model has been developed in order to simulate the mechanical behavior of non-circular chainring, especially the teeth. The aim is to use this finite element model as design tool to avoid teeth failure of non-circular composite chainring. In order to validate the model construction, results obtained with a circular aluminum chainring were compared with the literature. Then, the model was extended to non-circular composite chainring and the influence of the shape was studied. Due to the shape of the non-circular chainring, three load cases needed to be investigated. Non-circular composite chainring strength and damage scenario was detailed in function of the loading position.

II. Model Construction and Validation

A. Model Construction and Hypothesis

Two different chainrings were compared in this study, a

Dr. L. Mezeix is lecturer with the University of Burapha, Chonburi 20131 Thailand (corresponding author, phone: +66-957-621-81; fax: +663-874-5806; e-mail: laurentm@eng.buu.ac.th).
A. Elmikaty is master's student with University of Toulouse III, France, Toulouse 31077 France. (e-mail: abdelrahmanelmikaty@hotmail.com).
Z. Thanawarothon is Ph.D student in the Mechanical Engineering Department, University of Burapha, Chonburi 20131 Thailand, (e-mail: zhorth@gmail.com).

circular chainring of diameter 130 mm with 34 teeth (Fig. 2 (a)), and a non-circular chainring with 53 teeth (Fig. 2 (b)). The thickness is 2 mm for both parts. The radius of the non-circular chainring depended of the angle θ (Fig. 2 (b)) and is detailed in Table I. Teeth design proposed by Wang was used for both chainrings [21]. The chain consisted of rollers, inner and outer plates (Fig. 3), and it was provided by SRAM (reference PC-991). Roller diameter was 7.77 mm (0.306 in) and the chain pitch was 12.7 mm (0.5 in).

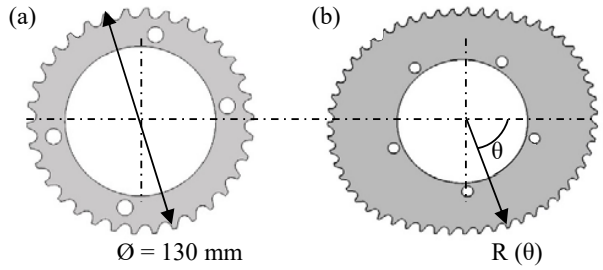

Fig. 2 Geometry of (a) circular and (b) non-circular chainring

TABLE I
RADIUS, R, OF THE NON-CIRCULAR CHAINRING IN FUNCTION OF THE ANGLE Θ

Angle, θ [°]	R [mm]	Angle, θ [°]	R [mm]
0	93.97	100	106.90
10	95.23	110	106.94
20	96.77	120	105.79
30	98.59	130	101.24
40	100.54	140	97.05
50	102.50	150	94.11
60	104.25	160	92.99
70	105.58	170	93.13
80	106.38	180	93.97
90	106.73		

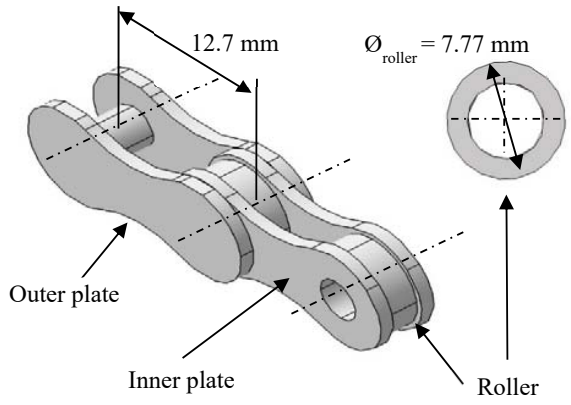

Fig. 3 Chain geometry

The FE model consisted of the chainring and a part of the chain all modelled with 794631 C3D8R solid elements. Literature showed that the loading is mainly concentrated on the first seven teeth [22]. Thus, in this paper, the first eleven rollers were simulated in order to reduce the computing time (Fig. 4). Moreover the mesh around these eleven rollers was refined to obtain more accurate results (Fig. 5). To simulate the chainring bolt (Fig. 1 (a)), encastré boundary condition was used (Fig. 4). Normal behavior was used as contact property in ABAQUS between the chain and the chainring. The scope of this work was the quasi-static mechanical strength of non-circular chainring and so friction between teeth and the chairing was not considered in this work. Due to the shape of the non-circular chainring three chain positions were investigated (Fig. 4), while for the circular chainring only one position was studied. The chain was assumed to be stretched and tangential loading representing its tension force was applied on (Fig. 4).

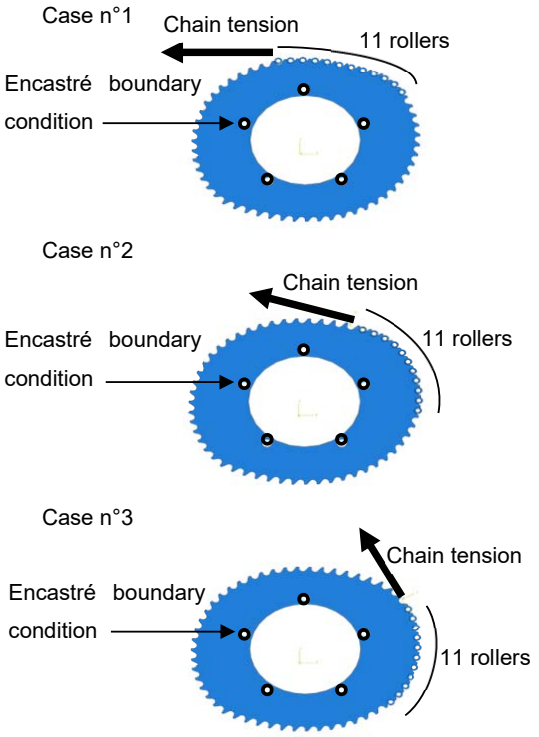

Fig. 4 Loading positions for non-circular chainring

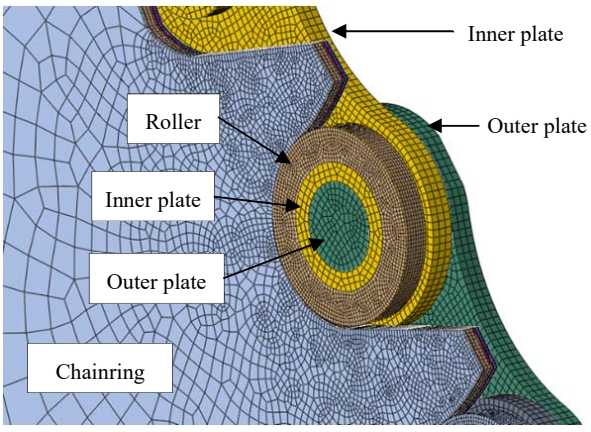

Fig. 5 View cut of the chain and chainring numerical simulation with mesh detail

B. Materials

The chain was made from steel (Table II) while the chainring was made in carbon 2/2 twill woven/epoxy ply (Table III). Two different stacking of 11 plies each were used [30/60/0/60/30/0/30/60/0/60/30] and [45_2/0/45_2/0/45_2/0/45_2]. Composite failure was simulated thanks to Hashin's criteria [23]. Hashin's criteria is a well-known criteria used in aerospace [6], [7], [24]. Indeed, edge damage on CFRP woven for aeronautical structures was successfully numerically predicted using Hashin's criteria and numerical results matched with experiments [25]. The Hashin's criterion is given by (1):

$$\left(\frac{\sigma_t}{\sigma_t^{f,t}}\right)^2 + \frac{\tau_{lt}^2 + \tau_{tz}^2}{\left(\tau_{lt}^f\right)^2} = 1 \quad (1)$$

where σ_t, τ_{lt} and τ_{tz} are respectively the transverse stress, the shear stress in the (l,t) plane and the shear stress in the (t,z) plane, evaluated in the neighboring volume elements, $\sigma_t^{f,t}$ the transverse failure stress in tension and τ_{lt}^f the failure shear stress [6]. The element stiffness becomes zero when the failure criterion is reached. Thus, the FE model employed explicit integration scheme in ABAQUS. Metallic behaviors were modelled using isotropic elastic laws behaviors, while the composite chainring were programmed using FORTRAN and input to ABAQUS in the form of a 'user material' (VUMAT) subroutine.

TABLE II
HSS STEEL [26] AND ALUMINUM [27] PROPERTIES

Material	E [GPa]	η	σy [MPa]
Steel AISI 4140	210	0.30	415
Aluminum 7075t6	71	0.33	521

TABLE III
CARBON 2/2 TWILL WOVEN /EPOXY PLY PROPERTIES

Carbon 2/2 twill woven /epoxy ply (T300/EPOTEC 535 LV, TH 7253 - 8)	
Longitudinal Young's modulus, El	35 GPa
Transverse Young's modulus, Et	35 GPa
Shear modulus, Glt	4.3 GPa
Poisson's ratio	0.05
Density, ρ	1700 kg/m^3
Failure	
Longitudinal tensile strength, $\sigma_l^{f,t}$	800 MPa
Transverse tensile strength, $\sigma_t^{f,t}$	800 MPa
In-plane shear strength, τ_{lt}^f	98 MPa
Out-of-plane shear strength, τ_{tz}^f	50 MPa

Chainring is subjected to different loading cases in function of the cycling motion (Fig. 6). For a standard 80 kg person the tension in the chain is only 500 N for cruising cycling which is considered to be representative of a cyclist's power output of 200 W [28]. The tension reaches 800 N for an amateur cyclist, i.e. power output of 300 W [28]. For the best professional cyclist the tension force in the chain can reach 1800 N that corresponds to a power output of 600 W [29]. Thus, in this study 800 N was considered as the Limit Load (LL) and 1800 N as the Ultimate Load (UL) (Fig. 6). Until LL, Hashin's criteria had to be lower than 1. From LL to UL composite damage tolerance concept was used [1, 30-32].

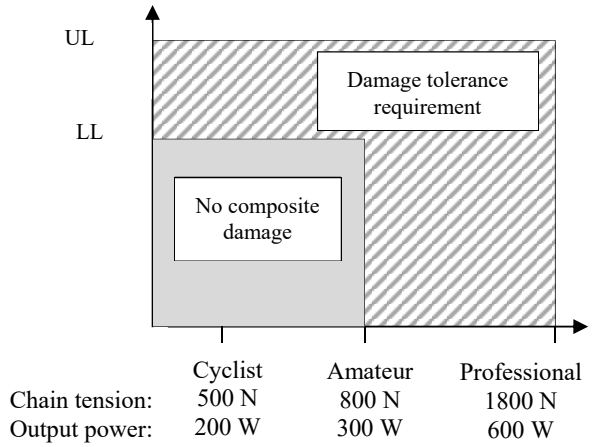

Fig. 6 Loading cases and failure criteria associated to cycling condition

C. Model Validation

In order to validate the numerical simulation (boundaries conditions, contact definition, mesh, elements properties…), evolution of the normalized maximum Von Mises stresses in the different teeth was plotted for the circular aluminum (Table II) chainring (Fig. 7). To isolate the geometrical effect, the data were condensed onto a single plot by normalizing the maximum Von Mises stress for a given tooth with respect to the maximum Von Mises stress of the first teeth. As observed, the simulation results replicate the stress distribution mentioned in the literature [22]. It is characterized by a large drop of the stress from the first to the fourth teeth where the stress is only 20% of the maximum. From the seventh tooth the stress is lower than 5% of the maximum. Finally, as the numerical model reproduced the stress distribution, it can be extended to non-circular chainring.

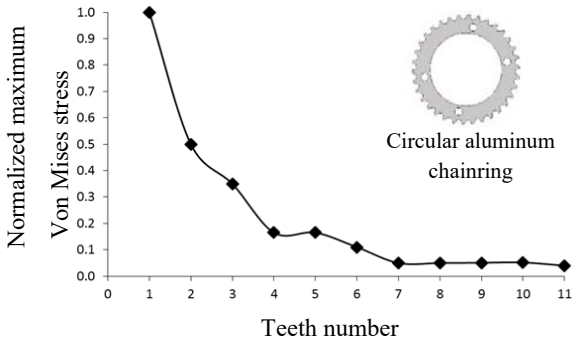

Fig. 7 Normalized maximum Von Mises stress distribution in function of the teeth number for the aluminum circular chainring and for the LL of 800 N

III. Results and Discussions

A. Failure Load

Numerical simulation was then used to predict the failure of non-circular composite chainring. The same numerical simulation, i.e. boundaries conditions, elements, mesh and contact was used. Effect of the stacking was investigated through [30/60/0/60/30/0/30/60/0/60/30] and [45_2/0/45_2/0/45_2/0/45_2] lay-up. Structural and final failures are presented in the Fig. 8. Structural failure was defined as the first damage given by the Hashin's criteria and had to appear for a chain force of, at least, 800 N defined as the LL (Fig. 6). Hashin's criterion was chosen because it showed its ability to predict the carbon/epoxy woven edge damage [26]. Final failure was defined as the maximum force the chainring could support and had to be for a chain tension of, at least, 1800 N defined as UL (Fig. 6).

Even for the structural and final failure, and whatever the loading position (Fig. 4), the [30/60/0/60/30/0/30/60/0/60/30] lay-up give better results than the [45_2/0/45_2/0/45_2/0/45_2] lay-up. Indeed, its structural failure for the case 2 and 3 is largely higher than those for [45_2/0/45_2/0/45_2/0/45_2] lay-up, while no stacking influence is observed for the case 1. Moreover, the [45_2/0/45_2/0/45_2/0/45_2] lay-up presents a structural failure lower than the LL for the case 2 and 3. Finally, for this lay-up, the final failure load of the case 3 is lightly higher than the UL.

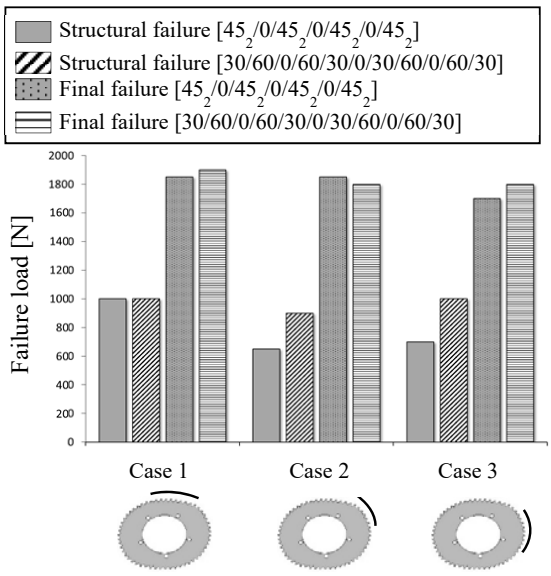

Fig. 8 Structural and final failure of non-circular composite chainring

B. Failure Scenario

Thanks to the evolutions of the force reaction the failure scenario of the composite non-circular chainring can be plotted for the three loading positions (Figs. 9-11). Whatever the loading position, the curve indicates a first linear domain (1) corresponding to the contact between the first roller and the first tooth only (Fig. 9). Then, the reaction force oscillates due to the successively contact between the different rollers and the associated teeth (2). The first damage, defined as the structural failure, is always located in the first tooth (3). Due to its failure the reaction force brutally decreases and the tension load starts being distributed to the others teeth and thus the force increases again until the next teeth failures (4 and 5). Finally, final failure occurs when the last tooth, i.e. 11th tooth fails (6).

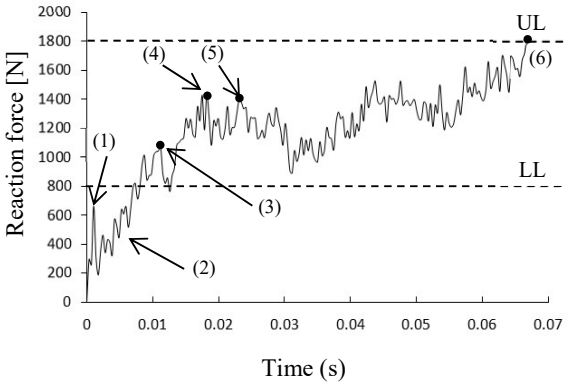

Fig. 9 Reaction force of non-circular composite chainring and for the loading position 1

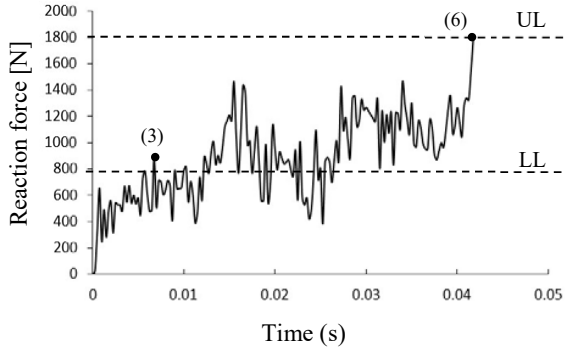

Fig. 10 Reaction force of non-circular composite chainring and for the loading position 2

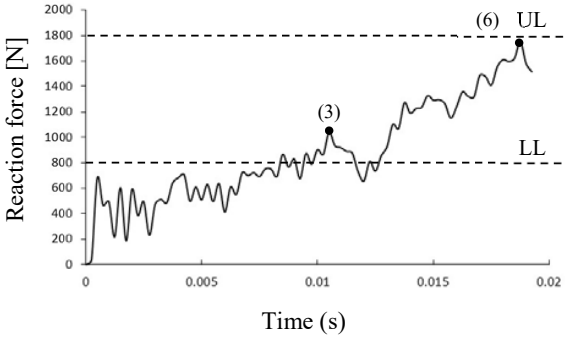

Fig. 11 Reaction force of non-circular composite chainring and for the loading position 3

Structural and final failure of the first tooth for the [30/60/0/60/30/0/30/60/0/60/30] lay-up, and for the loading position 3, are presented as representative failure profile in the

Fig. 12. As the lay-up is symmetrical, only half is presented and elements where Hashin's criteria reach 1, i.e. element failure, are highlighted in red. Initial failure starts in the plies in the center of the lay-up (Fig. 12 (a)). Moreover, the failure initiation is located on teeth surface in contact with the roller and cracks start on the fillet of the front surface of the tooth. Then, cracks propagate until the final failure (Fig. 12 (b)).

The specific teeth failure location failure of the non-circular composite chainring with the $[45_2/0/45_2/0/45_2/0/45_2]$ lay-up (Fig. 1 (a)) has been identified thanks to the numerical simulation. Indeed, final failure is due to the first teeth failure of the case 3 loading only (Fig. 9). Finally, the [30/60/0/60/30/0/30/60/0/60/30] lay-up provides better performance and it is a good lay-up for a non-circular composite chainring to avoid teeth failure.

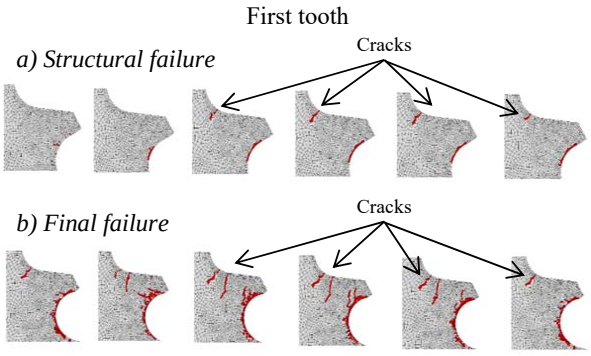

Fig. 12 Hashin's criteria for (a) structural and (b) final failure for the first tooth

IV. Conclusion

In order to design non-circular composite chainrings, especially to predict the teeth failure, a numerical simulation has been proposed. The chainring and a part of the chain have been modelled using an explicit simulation. Three loading positions were performed in order to study the effect of the non-circular chainring shape. CFRP made of 11 plies of carbon woven/epoxy were investigated, and Hashin's criterion has been used as failure criteria. Moreover, LL and UL corresponding to a chain tension of 800 N and 1800 N respectively were used as specification. According to the numerical simulation, the mechanical behavior of the non-circular composite chainring can be concluded as follows:

a) The first failure load for the $[45_2/0/45_2/0/45_2/0/45_2]$ lay-up is higher than the LL only for the case 1. However, the final failure occurs only for the case 3 that is corresponded to the observation made on specimens.
b) Damage scenario has been determined. First composite failure initiates in the first tooth and then propagates from the 1st to the 11th tooth. No effect of the non-circular shape has been demonstrated on the failure scenario. Indeed, cracks start always on the surface with the roller and on the fillet of the opposite tooth surface.
c) Composite non-circular chainring made with [30/60/0/60/30/0/30/60/0/60/30] lay-up gives better performance than with $[45_2/0/45_2/0/45_2/0/45_2]$ lay-up.

Non-circular composite chainring can carry the UL but the lay-up must be carefully chosen in order to avoid the non-circular chainring collapse. For a $[45_2/0/45_2/0/45_2/0/45_2]$ lay-up failure is due only to the breaking of the first teeth of the loading case 3. Therefore, [30/60/0/60/30/0/30/60/0/60/30] lay-up is advised. Ply snatching observed on specimen is probably due to impact of the chain on the chainring. Indeed, when cyclist shifts gear the chain can impact chainring teeth and, in the case of CFRP part, could damage it and reducing its strength. Experimental work on non-circular CFRP chainring is currently in progress to validate the numerical simulation and effect of the damage created by the chain impact is also under investigation.

References

[1] C. Bouvet, S. Rivallant, "Damage tolerance of composite structures under low-velocity impact," *in Dynamic Deformation, Damage and Fracture in Composite Materials and Structures*, 1st ed. Ed. V. Silberschmidt, 2016, pp. 7-33.
[2] B. Ostré, C. Bouvet, C. Minot, J. Aboissière, "Experimental analysis of CFRP laminates subjected to compression after edge impact," *Compos Struct*, vol. 152, pp. 767-778, September 2016.
[3] H. Abdulhamid, C. Bouvet, L. Michel, J. Aboissière, C. Minot, "Experimental study of compression after impact of asymmetrically tapered composite laminate." *Compos Struct*, vol. 149, pp. 292-303, August 2016.
[4] S. Rivallant, C. Bouvet, N. Hongkarnjanakul, (2013) "Failure analysis of CFRP laminates subjected to compression after impact: FE simulation using discrete interface elements." *Compos Part A: Appl Sci Manuf*, vol. 55, pp. 83-93, December 2013.
[5] C. Bouvet, L. Michel, J. Aboissiere, C. Minot, "Numerical simulation of impact and compression after impact of asymmetrically tapered laminated CFRP," *Int J Impact Eng*, vol. 95, pp. 154-164, September 2016.
[6] N. Hongkarnjanakul, C. Bouvet, S. Rivallant, "Validation of low velocity impact modelling on different stacking sequences of CFRP laminates and influence of fibre failure," *Compos Struct*, vol. 106, pp. 549-559, December 2013.
[7] B. Ostré, C. Bouvet, C. Minot, J. Aboissière, "Edge impact modeling on stiffened composite structures," *Compos Struct*, vol. 126, pp. 314–328, August 2015
[8] B. Ostré, C. Bouvet, C. Minot, J. Aboissière, "Finite element analysis of CFRP laminates subjected to compression after edge impact," *Compos Struct*, vol. 153, pp. 478-489, October 2016.
[9] N. Li, P. H. Chen, "Experimental investigation on edge impact damage and Compression-After-Impact (CAI) behavior of stiffened composite panels," *Compos Struct*, vol.138, pp. 134-150, March 2016.
[10] A. Mosallam, J. Slenk, J. Kreiner, "Assessment of residual tensile strength of carbon/epoxy composites subjected to low-energy impact," *J Aerosp Eng*, vol. 21, no. 4, pp. 249–258, October 2008.
[11] H. Brody, "The physics of tennis. III. The ball-racket interaction," *Am J Phys*, vol. 65, no. 10, pp. 981-987, May 1997.
[12] S. R. Otto, M. Strangwood, "The quasi-static and dynamic testing of damping in golf clubs shafts fabricated from carbon fibre composites," *Proced Eng*, vol. 2, no. 2, pp. 3361–3366, Jun 2010.
[13] P. Clifton, A. Subic, A. Mouritz, "Snowboard stiffness prediction model for any composite sandwich construction," *Proced Eng*, vol. 2, no. 2, pp. 3163-3169, Jun 2010.
[14] Staff "First Full Carbon Fiber Bike. High Performance Composites," *http://www.compositesworld.com/articles/ultralight-carbon-fiberepoxy-road-bike-from-kestrel*. Accessed 3 January 2004.
[15] T. Jin-Chee Liu, H. C. Wu, "Fiber direction and stacking sequence design for bicycle frame made of carbon/epoxy composite laminate," *Mater Des*, vol. 31, no. 4, pp. 1971-1980, April 2010.
[16] F. Ohlsson, "SwiftCarbon unveils lightweight frame reinforced by TeXtreme," Reinforced Plastics,"

http://www.textreme.com/news/swiftcarbon-unveils-lightweight-frame-reinforced-by-textreme. Accessed 12 May 2016.
[17] F. Höchtl, Hein M, Klug S, Sennera V "On the effect of chain stay impact on the structural safety of CFRP structures in mountain biking," *Proced Eng*, vol. 34, pp. 664-669, 2012.
[18] R. R. Bini, F. Dagoese, "Non circular chainrings and pedal to crank interface in cycling: a literature review," *Brazilian J Kinantropometry Hum Perform*, vol. 14, no. 4, pp. 470–482, January 2012.
[19] J. W. Rankin, R. R. Neptune, "A theoretical analysis of an optimal chainring shape to maximize crank power during isokinetic pedaling," *J Biomech*, vol. 41, pp. 1494–1502, April 2008.
[20] J. C. Martin, S. M. Lamb, N. A. Brown, "Pedal trajectory alters maximal single-leg cycling power," *Med Sci Sports Exerc*, vol. 34, no. 8, pp. 1332–1336, August 2002.
[21] Y. Wang, D. Ji, K. Zhan, "Modified sprocket tooth profile of roller chain drives," *Mech theor*, vol. 70, pp. 380-393. December 2013.
[22] J. Huo, Yu S, J. Yang, T. Li, "Static and Dynamic Characteristics of the Chain Drive System of a Heavy Duty Apron Feeder," *Open Mech Eng J*, vol. 7, pp. 121-128, November 2013.
[23] Z. Hashin, "Failure criteria for unidirectional fibre composites," *J Appl Mech*, vol. 47, no. 2pp. 329–334, Jun 1980.
[24] C. Bouvet C, S. Rivallant, J. J. Barrau, "Low velocity impact modeling in composite laminates capturing permanent indentation," *Compos Sci Technol*, vol. 72, no. 16, pp. 1977–1988, November 2012.
[25] K. C. Warren, R. A. Lopez-Anido, S. S. Vel, H. H. Bayraktar, "Progressive failure analysis of three-dimensional woven carbon composites in single-bolt, double-shear bearing," *Compos Part B*, vol. 84, pp. 266-276, January 2016.
[26] Azom, "AISI 4140 Alloy Steel (UNS G41400)," *Azo Materials*, http://www.azom.com/article.aspx?ArticleID=6769, 13 September, 2012.
[27] A. R. Torabi, M. Alaei, "Mixed-mode ductile failure analysis of V-notched Al 7075-T6 thin sheets," *Engineering Fracture Mechanics*, vol. 150, pp. 70–95. December 2015.
[28] A. Vayer, "La pleine puissance en cyclisme. Guide d'entraînement basé sur les données de puissance et de fréquence cardiaque, pour les débutants et les professionnels," in *Librairie Anglet*, 1st ed. Ed. Polar France, 2002, pp. 1-101.
[29] W. Fotheringham, "Team Sky data shows Chris Froome Tour climb was exceptional but normal," *The Gardian*. https://www.theguardian.com/sport/2015/jul/21/team-sky-data-chris-froome-tour-de-france, 21 July, 2015.
[30] M. Calomfirescu, F. Daoud, T. Puhlhofer, "A new look into structural design philosophies for aerostructures with advanced optimization methods and tools," In *IV European Conference Computational Mechanics*, Paris, 2010.
[31] J. Rouchon, "Certification of large airplane composite structures, recent progress and new trends in compliance philosophy," in *Proc. 17th Congress of the International Council of the Aeronautical Sciences*, Stockholm, 1990, pp. 1439-1447.
[32] Joint Airworthiness Requirements 25 (JAR25), part 1 requirements, part 2 acceptable means of compliance and interpretations, composite structures: JAR25 x 25.603 and ACJ 25.603.

L. Mezeix was born in France in 1981. He obtained his Bachelor of Mechanical Engineering from University of Rennes-1, Rennes, France in 2005. Then he obtained his Master of Science in Material Science from the University of Paul Sabatier, Toulouse, France in 2007. Finally, he obtained his PhD in Material Science and Engineering and Mechanical Engineering from the University of Toulouse III, Toulouse, France in 2010.

After his PhD he worked 2 years as Research and Development Engineer for Sogelair Aerospace in France where he worked on composite structure development for aircraft. Then, he travelled to Malaysia where he worked 2 years as Post-Doctoral under Aerospace Malaysian Innovation Center (AMIC) project on composite spring back prediction for aircraft structures. Currently he works as Lecturer at Burapha University and as Aerospace Engineer with Geo-Informatics and Space Technology Development Agency (GISTDA), both in Chonburi, Thailand. He focuses on composite for aerospace applications.

A. Elmikaty was born in Egypt in 1992. He obtained his Bachelor of Aerospace Mechanical Engineering from University of Paul Sabatier, Toulouse, France in 20014. Then he obtained his Master of Engineering in Aeronautical Mechanics from the University of Paul Sabatier, Toulouse, France in 2017.

Z. Thanawarothon was born in Thailand in 1975. He obtained his Bachelor of Mechanical Engineering from King Mongkut's Institute of Technology Ladkrabang, Bangkok, Thailand in 1997. Then he obtained his Master of Engineering in Mechanical Engineering from King Mongkut's Institute of Technology Ladkrabang, Bangkok, Thailand in 2003. Then, he joined as Area MANGER the company GJ Steel Public Company Limited. In 2015, he started PhD in Mechanical Engineering in the University of Burapha, Chonburi, Thailand. His PhD focus on the development of non-circular composite chainring.